TCR Repertoire, Clonal Dominance, and Pulmonary Trafficking of Mycobacterium-Specific CD4+ and CD8+ T Effector Cells in Immunity Against Tuberculosis

George Du, **Crystal Y. Chen**, **Yun Shen**, **Liyou Qiu**, **Dan Huang**, **Richard Wang**, and **Zheng W. Chen**

Department of Microbiology and Immunology, Center for Primate Biomedical Research, University of Illinois College of Medicine, Chicago, IL 60612

Abstract

Clonal responses of *Mycobacterium tuberculosis*-specific CD4+ or CD8+ T effector cells producing antituberculosis cytokine IFN-γ in the context of immune protection against tuberculosis remain poorly characterized in humans. Utilizing decade-long TCR expertise, we previously developed a useful method to isolate clonotypic TCR sequences from Ag-specific IFN-γ–producing T cells and to specifically measure clonotypic TCR frequencies in the T cell pool. In this study, we investigated TCR Vβ repertoires/CDR3 usage, clonal expansion or dominance, and pulmonary trafficking or accumulation for purified protein deritative (PPD)-specific T effector cells producing IFN-γ during bacillus Calmette-Guérin (BCG) vaccination and subsequent *M. tuberculosis* challenge of macaques. We found that while PPD-specific CD4+ and CD8+ T effector clones employed diverse TCR Vβ repertoires, 30–33% of IFN-γ+CD4+ T cell clones from three *M. tuberculosis*-infected macaques expressed TCR bearing a conserved residue leucine in CDR3. Many Ag-specific IFN-γ+ CD4+ and few CD8+ T effector cells emerged as dominant clones during mycobacterial infections and underwent major recall expansion after pulmonary *M. tuberculosis* infection of BCG-vaccinated macaques. PPD-specific T cell clones readily trafficked to the airway or lung after BCG vaccination or *M. tuberculosis* infection, and some of them continuously accumulated in lungs during *M. tuberculosis* infection even after they became undetectable in the circulation. Importantly, remarkable recall expansion and pulmonary accumulation of T effector cells coincided with BCG-induced protection against tuberculosis. Thus, rapid clonal expansion and pulmonary accumulation of Ag-specific T effector cells appear to be one of the immune mechanisms underlying immunity against tuberculosis.

Tuberculosis (TB) remains one of the major causes of global mortality, and it has become increasingly prevalent and deadly as a result of the HIV/AIDS pandemic and the emergence of extensively drug resistant strains of *Mycobacterium tuberculosis* (1). Precise protective elements in immunity against human TB are poorly characterized, although HIV-mediated CD4+ T cell deficiency clearly increases the susceptibility to TB (2–4). Elucidating precise immune elements for controlling human TB is therefore of central importance for ultimately developing a better vaccine and immunotherapeutic against TB and for reducing TB

Address correspondence and reprint requests to Dr. Zheng W. Chen, Department of Microbiology and Immunology, Center for Primate Biomedical Research, University of Illinois College of Medicine, 835 S. Wolcott Avenue, MC790, Chicago, IL 60612. zchen@uic.edu.

G.D. and C.Y.C. contributed equally to this work and share the first authorship.

epidemics. It is widely accepted that CD4^{+} T cells play an important role in the ability of humans and experimental animals to resist active *M. tuberculosis* infection (5–8). In this regard, Th1 cytokine IFN-γ has been shown to be crucial for immune protection against TB in mice (9, 10). Our recent study has also demonstrated that vaccine-elicited CD8^{+} T cells play a critical role in immunity against active TB (11). However, clonal responses and potential lung-trafficking of *M. tuberculosis*-specific CD4^{+} or CD8^{+} T effector cells producing anti-TB cytokine IFN-γ in the context of anti-TB immunity remain poorly characterized in humans (12–14). Studies of Ag-specific T cells for TCR repertoires/CDR3 usage, clonal expansion, and pulmonary trafficking in immunity against TB should help to elucidate immune mechanisms for protective T cell immune responses.

We have recently used our decade-long TCR expertise and developed a useful method to isolate TCR VDJ clonotypic sequences from a limited number of purified protein deritative (PPD)-specific IFN-γ–producing T cells and to specifically measure clonotypic TCR frequencies in the T cell pool using the PCR-based real-time quantitation (15). The real-time quantitation technique using clonotypic primers specifically quantitates a target clonotypic TCR clone at a detection limit of 10^{-5} Ag-specific T cells, and it discriminates other clones that differ by two or more bases in DJ regions (15). Employing this useful method, we investigated TCR Vβ repertoires/CDR3 usage, clonal expansion or dominance, and pulmonary trafficking or accumulation for PPD-specific T effector cells producing anti-TB cytokine IFN-γ during bacillus Calmette-Guérin (BCG) vaccination and subsequent *M. tuberculosis* challenge of macaques. We found that while PPD-specific T effector clones employed diverse TCR Vβ repertoires, 30–33% of IFN-γ^{+} CD4^{+} T cell clones from three *M. tuberculosis*-infected macaques expressed TCR bearing a conserved residue leucine in CDR3 despite different Vβ usage. Many CD4^{+} and few CD8^{+} T effector clones emerged as dominant clones during BCG vaccination and underwent major recall expansion and trafficking to the airway after *M. tuberculosis* infection. Such major recall expansion and rapid pulmonary accumulation coincided with BCG-induced anti-TB immunity.

Materials and Methods

Macaque animals

A total of eight juvenile Indian rhesus macaques (2 y old) were used for evaluating clonal immune responses of *M. tuberculosis*-specific CD4^{+} and CD8^{+} T cells. Studies using all the animals were documented in animal protocols and approved by the Institutional Animal Care and Use Committee.

BCG vaccination and M. tuberculosis *challenge*

Two groups of juvenile Indian rhesus macaques (four animals per group) were vaccinated i.v. or intradermally (below) with 10_6 CFUs BCG (Pasteur strain) and saline control, respectively. One and one-half months later each of them was challenged with 400 CFUs *M. tuberculosis* H37Rv strain by aerosol as previously described (16). Four control naive animals became moribund and had to be euthanized due to the development of fatal tuberculosis within 1.5 mo after the infection, whereas the BCG-vaccinated macaques survived fatal tuberculosis during a 2.5-mo follow-up (16). The surviving macaques with transient low levels of bacillus but no evidence of active tuberculosis were then treated daily for 3 mo with anti-TB drugs; that is, isoniazid (5 mg/kg) and pyrazinamide (15 mg/kg) mixing with yogurt as previously described (17).

To optimally investigate Ag-specific T effector clones for pulmonary trafficking, two additional rhesus macaques received the first i.v. BCG vaccination and, 4 mo later, the second BCG vaccination. Ag-specific clonal responses were extensively followed for 6 mo.

Because BCG organisms were not detected in bronchoalveolar lavage (BAL) fluid without increases in neutrophils during the secondary BCG infection (Fig. 6), detection of Ag-specific clonotypic TCR clones in both blood and BAL fluid implicated the trafficking of T cells to the airway.

To examine if intradermal BCG vaccination was similar to i.v. BCG administration in inducing accumulation of T effector cells in the airway, four rhesus macaques were intradermally vaccinated with BCG and assessed for the occurrence of PPD-specific IFN-γ^+ T cells in BAL fluid (Fig. 7). The intradermal BCG vaccination appeared to be relevant somewhat to i.v. BCG administration, as T effector cell recall expansion and anti-TB immunity were also seen in adult rhesus macaques that received intradermal BCG vaccination (18), a standard vaccination route.

BAL

BAL was done essentially the same as previously described (11, 19, 20). Clear BAL fluid without blood contamination was used for evaluation of clonal T cell responses.

Sampling approaches

Two parallel approaches were employed to quantitate Ag-specific T cell clones in infection. To isolate clonotypic TCR and design clonotypic primers for real time quantitation, PBLs from *M. bovis* BCG-infected macaques were isolated from blood and used to generate Ag-specific T cells by means of peptide stimulation and intracellular IFN-γ staining. The Ag-specific IFN-γ– producing T cells were purified by flow sorting; TCR VDJ DNA was isolated by megaplex PCR and sequenced for designing clonotypic primers.

In parallel, 10×10^6 PBL or 3×10^6 BAL cells were collected and frozen in a liquid nitrogen tank over time after BCG vaccination and *M. tuberculosis* infection. The frozen cells were then used for RNA isolation and cDNA synthesis. cDNA and clonotypic primers were used to quantitate T cell clones during BCG vaccination and *M. tuberculosis* infection.

ELISPOT measuring PPD-specific IFN-γ–producing cells

PPD-specific IFN-γ^+ cells in PBMCs and BAL fluid were detected as we previously described (11, 18, 21, 22).

Intracellular cytokine staining and purification of PPD-specific IFN-γ$^+$ CD4$^+$ and CD8$^+$ T cells by flow cytometry sorting

Intracellular cytokine staining (ICS) for IFN-γ^+ cells in PBMCs was done as previously described (11, 15, 18, 22). Stained cells were fixed in 2% formaldehyde. IFN-γ^+ CD4$^+$CD3$^+$ T cells and IFN-γ^+ CD8$^+$CD3$^+$ T cells were then purified and enumerated by flow cytometry sorting, essentially as we previously described (15, 23). The formaldehyde-fixed PPD-specific CD4 T cells were subjected to TCRVDJ DNA isolation using the megaplex PCR.

Isolation of clonotypic TCR VDJ DNA from formaldehyde-fixed PPD-specific CD4$^+$ or CD8$^+$ T cells

To isolate and amplify TCR β VDJ DNA from formaldehyde-fixed cells, three-round nested PCRs (megaplex PCRs) were employed using DNA prepared from the sorted cells as well as three sets of 24 forward Vβ family-specific primers and three sets of 13 reverse Jβ primers as shown in Table 1 and Fig. 1 in Du et al. (15). The first and second round of nested megaplex PCRs were performed in a single PCR tube using external, middle sets of mixed 24 forward Vβ family-specific primers and mixed 13 reverse Jβ primers, respectively,

whereas the third megaplex PCR amplified and displayed clonotypic Vβ-D-Jβ DNA at the level of individual Vβ-Jβ recombinations for direct sequencing (15). The method allowed isolation clonotypic TCR DNA in fidelity from 20 to 2000 sorted cells (15). The extremely low frequencies of specific Teffector cells in three naive controls that died at an early stage precluded the clonotypic TCR sequence isolation and subsequent quantitation of TCR clones measured over time by real-time PCR.

Direct sequencing of TCR VDJ DNA

The individual clonotypic Vβ-D-Jβ DNA recovered from a gel extraction kit from Qiagen (Valencia, CA) was directly sequenced using the third-round PCR primers, as previously described (15). If the direct sequencing showed multiple templates, the DNA was then inserted into the plasmid SP65 (Promega, Madison, WI) for cloning and sequencing, as previously described (23).

Isolation of RNA from frozen cells and cDNA synthesis

Total RNA was isolated from PBLs using the TRIzol isolation method (15). The RNA pellet was resuspended in RNase-free deionized water and then used immediately for synthesis of cDNA using the protocol provided in the cDNA synthesis kit from Clontech Laboratories (Palo Alto, CA).

Real-time quantitative PCR for quantitating Ag-specific T cell clones

To quantitate clonotypic T cell clones in a T cell pool, individual clonotypic TCR transcripts were measured for their frequencies in total TCR β transcripts (Cβ) (15). This was done essentially the same as previously described (15). Forward Vβ family-specific primers and TaqMan probes for real-time quantitative PCRs were designed at the region close to the 3′ end of Vβ regions; Jβ clonotypic reverse primers were designed based on the unique sequences in D-J regions [please see Table 1b, 1c in Du et al. (15)]. The real-time quantitative PCR was performed using PE Applied Biosystems 7700 single reporter Sequence Detection Systems 1.6.3 (Applied Biosystems, Foster City, CA) as we previously described (15). All data were analyzed using the GeneAmp 7700 SDS software (Applied Biosystems).

To standardize expression levels of Vβ and Cβ transcripts, C_T Vβ and C_T Cβ were verified by C_T values for a housekeeping gene, β-actin (C_T β-actin) (15). The expression levels of individual clonotypic TCR transcripts among a total of TCR β transcripts within the sample were then calculated using the formula, $2^{-[(C_T\,V\beta\,-\,C_T\,\beta\text{-actin})\,-\,(C_T\,C\beta\,-\,C_T\,\beta\text{-actin})]}$, as we and others previously described (15, 24–26). The calculation gave rise to the ratio of clonotypic Vβ-bearing transcripts versus Cβ transcripts (15). The data were then expressed as a relative expression of Ag-specific IFN-γ–producing T cell clones, (Vβ transcripts/Cβ transcripts) $\times$ 10^5 (15). Such an expression of data was based on the consideration that the expression levels of clonotypic VβDJβ-bearing transcripts were always less than those of Cβ transcripts, and that the detection limit for Ag-specific T cell clones in our assay system was 10^{-5} cells (15).

Statistical analysis

Statistical analysis was done using a Student *t* test, as previously described (16).

Results

PPD-specific CD4^{+} and CD8^{+} T effector clones employed diverse TCR Vβ repertoires; 30–33% of IFN-γ^{+} CD4^{+} T cell clones from three M. tuberculosis-infected macaques expressed TCR bearing a conserved residue leucine in CDR3

TCR Vβ repertoire and clonotypic sequences of *M. tuberculosis*-specific T effector cells producing anti-TB cytokine IFN-γ remain incompletely known (12–14). Because IFN-γ is one of the major T effector cytokines contributing to anti-TB immunity (9, 10), we sought to determine the breadth and clonotypes of Ag-specific IFN-γ[+] T effector cells using our validated method for TCR isolation and extensive TCR Vβ repertoire/CDR3 analyses (15, 23, 27–29). PPD-specific IFN-γ^{+} cells in PBLs were detectable after BCG vaccination and *M. tuberculosis* infection (Fig. 1*A*). CD4^{+} and CD8^{+} T cells in PBLs were reproducibly detected by ICS at week 5 after pulmonary *M. tuberculosis* infection of macaques (Fig. 1*B*) (18, 22). These *M. tuberculosis*-specific T effector cells were therefore isolated by flow cytometry sorting as we described previously (15, 23) and were assessed for TCR Vβ families and clonotypic CDR3 sequences by taking advantage of the recombined VDJ DNA derived from the isolated cells (15). Notably, *M. tuberculosis* PPD-specific IFN-γ^{+} CD4^{+} and CD8^{+} T effector cells in *M. tuberculosis*-infected macaques employed multiple TCR Vβ families during primary *M. tuberculosis* infection of naive or BCG-vaccinated macaques (Fig. 2). These Ag-specific T effector cells in each macaque often expressed selected TCR comprised of 4–11 Vβ family genes and diverse CDR3 sequences/lengths (Fig. 2). However, some Vβ families were predominantly used for recognition of MHC/peptide complexes despite the fact that their CDR3 sequences and lengths were not identical (Fig. 2). Interestingly, 30–33% of IFN-γ^{+}CD4^{+} T cell clones from three infected macaques (Mm3055, Mm2995, and Mm3050) expressed TCRs bearing a conserved residue leucine in the N-D junctional region (Fig. 2). Although many clones sharing the leucine residue in CDR3 were not dominant clones, the data suggested a selection by potentially conserved MHC class II/peptide complexes. Thus, while PPD-specific T effector clones employed diverse TCR Vβ repertoires during *M. tuberculosis* infection, some IFN-γ^{+}CD4^{+} T cell clones could express TCRs bearing a conserved residue leucine in CDR3.

Many Ag-specific IFN-γ^{+} CD4^{+} and few CD8^{+} T effector cells emerged as dominant clones during mycobacterial infections and underwent major recall expansion after pulmonary M. tuberculosis *infection of BCG-vaccinated macaques*

Once we isolated clonotypic TCR sequences of PPD-specific IFN-γ^{+} CD4^{+} and CD8^{+} T effector cells, we sought to determine frequencies of these individual T effector clones over time after pulmonary *M. tuberculosis* infection. We used PCR-based real-time quantitation to measure the frequencies of these clones in cDNA derived from PBLs collected and frozen after BCG vaccination and subsequent *M. tuberculosis* infection. The real-time quantitation of each T cell clone was done using a 5′-Vβ–specific primer and a 3′-clonotypic primer corresponding to the unique sequence in the D+N and J (start) region as we previously described (15).

A number of TCR transcripts of CD4^{+} T effector cells were readily quantitatable or measurable 2–3 wk after i.v. BCG infection or pulmonary *M. tuberculosis* infection (Fig. 3). The occurrence of these measurable clones indicated a clonal expansion of the dominant T effector cell clones. However, many T cell clones were at low frequency and unquantitatable due to the detection limit for the PCR-based real-time quantitation (Fig. 3) (15). Interestingly, a number of T cell clones measurable after BCG infection were detected at higher frequencies in PBLs weeks after pulmonary *M. tuberculosis* infection (Fig. 3), whereas most clones from BCG-vaccinated macaques without *M. tuberculosis* infection became unquantitatable or at very low frequencies at 5–6 wk after BCG vaccination (15).

These contrasting data suggested that BCG-primed clones had undergone recall expansion after *M. tuberculosis* infection of the BCG-vaccinated macaques. Some clones undergoing recall expansion could increase up to 1000–3000 copies per 10^5 total TCR (Cβ) transcripts (Fig. 3). Notably, these increased clones were quite dynamic in the blood circulation over time after the infection (Fig. 3). Most clones became unquantitatable 2.5 mo after *M. tuberculosis* challenge (Fig. 3), presumably due to BCG-induced control of acute *M. tuberculosis* infection.

Six clonotypic TCR sequences representing CD8$^+$ T cell clones were also quantitatable, but only two of them were at a "sub-dominant" or "dominant" level in the blood after i.v. BCG infection or pulmonary *M. tuberculosis* infection (Fig. 3). The abundance of CD4$^+$ clones and the paucity of CD8$^+$ clones appeared to be consistent with the general idea that CD4$^+$ T cells constitute greater numbers of IFN-γ–producing cells than do CD8$^+$ T cells. We could not rule out the possibility that the CD8$^+$ paucity was also attributed to the fact that PPD used for ICS stimulation was less efficient than optimal 9- to 12-mer peptides to stimulate CD8$^+$ T cells that could be sorted by flow for clonotypic TCR sequence selection and subsequent frequency quantitation.

Thus, many Ag-specific CD4$^+$ T effector clones but few CD8$^+$ T clones emerged as dominant clones in mycobacterial infections, and they underwent major recall expansion after pulmonary *M. tuberculosis* infection of BCG-vaccinated macaques.

PPD-specific T cell clones readily trafficked to the airway after BCG vaccination or M. tuberculosis infection, and some of them continuously accumulated in lungs during M. tuberculosis infection even after they became undetectable in the circulation

Rapid accumulation of Ag-specific T effector cells in lungs may be critical for mounting anti-TB immunity after infection. Despite the fact that many T cells infiltrated into the lungs in forming granulomas during *M. tuberculosis* infection, it remains poorly characterized whether certain numbers of Ag-specific CD4$^+$ or CD8$^+$ T effector clones traffick to the pulmonary compartment after clonal expansion in lymphoid tissues. To address this, we first demonstrated that PPD-specific IFN-γ$^+$ T cells were detectable in the airway (BAL fluid) after pulmonary *M. tuberculosis* infection (Fig. 4). We then made use of the quantitatable (dominant) clonotypic TCR clones identified in the circulation as described above to determine whether they were measurable as well in the airway. Interestingly, at 8 d after *M. tuberculosis* infection, many dominant CD4$^+$ T effector clones expressing clonotypic TCR in PBLs were also detected at high frequencies in the airway, with two CD8$^+$ T clones having been detected at low levels (Fig. 5). The accumulation of these dominant PPD-specific IFN-γ$^+$ T cell clones in the airway was sustained at days 14, 25, 41, and 61 after pulmonary *M. tuberculosis* infection (Fig. 5). Some CD4$^+$ clones could accumulate at the frequency of up to 1000–5000 per 10^5 total TCR (Cβ) transcripts in the airway at days 14 and 41 despite some fluctuation for these clones (Fig. 5). Notably, at late time points some clones continuously accumulated in the airway despite the fact that they had already become undetectable for weeks in the blood (Vβ4Jβ1.5; Vβ4Jβ2.3 for 3055; Vβ8Jβ1.2 and Vβ21Jβ2.2 for 3050; Fig. 5).

To further investigate the airway trafficking of Ag-specific T effector clones, rhesus macaques immunized previously with BCG 4 mo earlier were vaccinated again with BCG and assessed for PPD-specific clonotypic T cell clones that had trafficked to the airway. While BCG organisms were not detected in BAL fluid, with no or few neutrophils found over time after the second BCG (Fig. 6; please see legend for the # symbol), we consistently found that PPD-specific clonotypic TCR clones identified in the circulation were also measurable in BAL cells over time after the second BCG vaccination (Fig. 6). In examining whether intradermal BCG vaccination was similar to i.v. BCG administration in inducing

accumulation of T effector cells in the airway, we found that accumulation of T effector cells in the airway was also induced by intradermal BCG vaccination (Fig. 7). The data suggested that both routes were comparable in this setting.

These results therefore suggested that PPD-specific IFN-γ^+ T cell clones could traffick to the airway after BCG vaccination or *M. tuberculosis* infection, and that some clones could continuously accumulate in the airway during *M. tuberculosis* infection even after they were no longer detectable in the peripheral blood.

Remarkable recall expansion and rapid pulmonary accumulation of T effector cells coincided with BCG vaccine-induced protection against fatal M. tuberculosis *infection*

Given the possibility that IFN-γ^+ CD4$^+$ and CD8$^+$ T effector cells in lungs contribute to anti-TB immunity, we sought to determine whether major recall expansion and pulmonary accumulation of PPD-specific T effector clones after *M. tuberculosis* infection of BCG-vaccinated macaques coincided with protection against TB (16). While naive juvenile Indian rhesus controls died of fatal *M. tuberculosis* infection, all BCG-vaccinated macaques survived with much lower *M. tuberculosis* burdens (16). Interestingly, the BCG vaccine-induced anti-TB immunity coincided with the major recall expansion of PPD-specific CD4$^+$ and CD8$^+$ T effector cells in the airway after *M. tuberculosis* challenge (Fig. 3). Importantly, the detectable protection was also associated with the high-frequency accumulation of those dominant T cell clones in the airway (Fig. 5). Comparative analysis of the PPD-specific IFN-γ^+ T effector cells between BCG-vaccinated macaques and naive controls also indicated that rapid major expansion of BCG-primed T effector cells was associated with protection against fatal TB (Fig. 8). It is also noteworthy that T effector cell recall expansion and anti-TB immunity were similarly seen in adult rhesus macaques that received intradermal BCG vaccination (18), a standard BCG vaccination route. Thus, clonal recall expansion and pulmonary accumulation of T effector clones appeared to contribute to BCG-induced anti-TB immunity.

Discussion

To our knowledge, the present study represents the first extensive experiment dissecting TCR repertoires/CDR3, clonal dominance/recall expansion, and pulmonary trafficking/accumulation for Ag-specific CD4$^+$ and CD8$^+$ T effector clones producing anti-TB cytokine IFN-γ during BCG vaccination and *M. tuberculosis* infection of nonhuman primates. A recent human study reported a marked CD8$^+$ T cell clonal expansion in the blood of children with TB, although Ag specificity, expansion versus time course, and pulmonary responses for these CD8$^+$ T cells were not known (13). Another human study identified highly focused responses of T cells in lungs in the latent *M. tuberculosis* infection (14). However, it would be interesting to see whether such responses are also apparent in primary *M. tuberculosis* infection or TB, and how these highly focused T cell responses are interrelated with the naturally presented epitopes and the TCR repertoires in the circulation or lymphoid tissues. Thus, our study extends human studies to provide further information regarding clonal immune responses of *Mycobacterium*-specific T effector cells in *M. tuberculosis* infection, particularly demonstrating that recall clonal expansion and rapid pulmonary accumulation of Ag-specific T effector cells closely correlate with vaccine-induced immunity against TB.

PPD-specific CD4$^+$ and CD8$^+$ T cells exhibited broad TCR repertoires involving multiple Vβ families and heterogeneous CDR3 sequences and lengths during *M. tuberculosis* infection. This might be due to the fact that PPD protein contains a number of epitopes that can be presented by different MHC class I and II alleles. In fact, we previously showed that even the Mamu-A*01–restricted CD8$^+$ T cell population recognizing an immunodominant

epitope indeed employed remarkably broad TCR repertoire during acute and chronic macaque SIV infection (23, 28).

Interestingly, 30–33% of PPD-specific CD4$^+$ T cell clones in three *M. tuberculosis*-infected macaques expressed TCR bearing a selected residue leucine at the CDR3 N-D junctional region despite the fact that they employed several different Vβ families. These results suggest that these CD4$^+$ T effector clones might share some TCR structural features required for recognition of a conserved peptide of PPD, and such a hypothetical peptide might serve as an immunodominant epitope selecting for the leucine-bearing TCRs expressed by the CD4$^+$ T effector cells. Further studies are needed to confirm TCR binding to a defined peptide/MHC complex.

Clonal expansion of PPD-specific CD4$^+$ and CD8$^+$ T effector clones could occur as early as 2–3 wk after i.v. BCG vaccination or pulmonary *M. tuberculosis* infection. Some of them sustained clonal expansion as dominant clones, whereas others were no longer quantitatable at later time points. The dynamic clonal representation in the circulation appears to be driven by cytokine environments, which are presumably different between acute and chronic infections. In fact, our earlier studies demonstrated that a number of epitope-specific T cell clones identified in acute SIV infection can lose their dominance in the circulation in chronic infection (23, 28).

Recall expansion of dominant CD4$^+$ T cell clones after *M. tuberculosis* infection of BCG-vaccinated macaques was remarkable, as clonotypic TCR transcript numbers of a CD4$^+$ T cell clone could increase to 3000 copies among 10^5 total TCR (Cβ) transcripts. The recall expansion of these T effector clones was likely stimulated by same epitope peptides derived similarly from BCG-and *M. tuberculosis*-infected macrophages or dendritic cells. More importantly, the recall expansion of these dominant clones correlated with BCG vaccine-induced immunity against fatal *M. tuberculosis* infection in the juvenile Indian rhesus macaques. Such findings suggest that these T effector clones contribute to the immune protection. This notion is indeed supported by our recent observation indicating that vaccine-elicited CD4$^+$ and CD8$^+$ T cells play a role in antimycobacterial immunity (18, 30).

Interestingly, animal Mm2762 had a log less clonal expansion than did the other immunized animals, but it also had the lowest bacterial burden. It is possible that low levels of clonal expansion may reflect susceptibility to *M. tuberculosis*, as it did in the unimmunized animals, but it can also reflect superior control of mycobacterial infection.

To our knowledge, our results provided the first clonotypic TCR evidence suggesting that some immunodominant T cell clones could traffick to lungs and continuously accumulate in the airway during *M. tuberculosis* infection. This presumption was implicated since the dominant clonal TCR sequences were identified and quantitated both in the circulation and airway. The observation was consistent with the recent human study demonstrating that Ag-specific T cells were detectable in lung biopsies in humans with latent *M. tuberculosis* infection (14). Although the human study was not able to link all expanded TCR Vβ families to the recognition of naturally processed and presented *M. tuberculosis* epitopes (14), our results clearly demonstrated that many Ag-specific CD4$^+$ but few CD8$^+$ T effector cells producing anti-TB cytokine IFN-γ could remarkably expand as dominant clones in both circulation and airway during *M. tuberculosis* infection. It is noteworthy that some dominant T effector clones could continuously accumulate in the airway even after these clones were no longer detectable in the blood circulation. The airway trafficking of Ag-specific T effector clones was also supported by the extensive follow-up study in the BCG-vaccinated macaques. Because there was no evidence of lung infection or damage in the BCG-vaccinated macaques (Fig. 6), Ag-specific T cell clones that accumulated in the airway

during the 6-mo period might be recruited through transendothelial trafficking or migration rather than due to the damage of lung tissues. This notion is indeed consistent with our previous observation that phosphoantigen-specific IFN-γ^+ Vγ2Vδ2 T effector cells can readily traffic to the airway after their peripheral activation even in the absence of lung infection or injury (19). The i.v. and intradermal BCG vaccinations appear to be somewhat relevant since both can elicit accumulation of T effector cells in the airway and induce anti-TB immunity (16, 18). It is important to note that although IFN-γ controls murine TB, human studies have not found a correlation between blood T effectors producing this cytokine and anti-TB immunity. Our data suggest that pulmonary recruitment of Ag-specific T effector cells may be the immune correlate of protection. Collectively, our findings suggest that Ag-specific CD4$^+$ and CD8$^+$ T cells can efficiently traffick to lungs from local or remote lymphoid tissues during BCG vaccination and *M. tuberculosis* infection. The pulmonary trafficking and accumulation of these dominant Ag-specific T effector clones producing anti-TB cytokine IFN-γ may contribute to the resistance to active TB.

Acknowledgments

Abbreviations used in this paper

BAL   bronchoalveolar lavage

BCG   *Mycobacterium bovis* bacillus Calmette-Guérin

D   days

ICS   intracellular cytokine staining

PPD   purified protein deritative

TB   tuberculosis

References

1. Wells CD, Cegielski JP, Nelson LJ, Laserson KF, Holtz TH, Finlay A, Castro KG, Weyer K. HIV infection and multidrug-resistant tuberculosis: the perfect storm. J. Infect. Dis. 2007; 196(Suppl. 1):S86–S107. [PubMed: 17624830]

2. Jones BE, Young SM, Antoniskis D, Davidson PT, Kramer F, Barnes PF. Relationship of the manifestations of tuberculosis to CD4 cell counts in patients with human immunodeficiency virus infection. Am. Rev. Respir. Dis. 1993; 148:1292–1297. [PubMed: 7902049]

3. Mukadi Y, Perriëns JH, St Louis ME, Brown C, Prignot J, Willame JC, Pouthier F, Kaboto M, Ryder RW, Portaels F, et al. Spectrum of immunodeficiency in HIV-1-infected patients with pulmonary tuberculosis in Zaire. Lancet. 1993; 342:143–146. [PubMed: 8101257]

4. Theuer CP, Hopewell PC, Elias D, Schecter GF, Rutherford GW, Chaisson RE. Human immunodeficiency virus infection in tuberculosis patients. J. Infect. Dis. 1990; 162:8–12. [PubMed: 1972384]

5. Boom WH, Canaday DH, Fulton SA, Gehring AJ, Rojas RE, Torres M. Human immunity to *M. tuberculosis*: T cell subsets and antigen processing. Tuberculosis (Edinb.). 2003; 83:98–106. [PubMed: 12758197]

6. Kaufmann SH. How can immunology contribute to the control of tuberculosis? Nat. Rev. Immunol. 2001; 1:20–30. [PubMed: 11905811]

7. Shen Y, Zhou D, Chalifoux L, Shen L, Simon M, Zeng X, Lai X, Li Y, Sehgal P, Letvin NL, Chen ZW. Induction of an AIDS virus-related tuberculosis-like disease in macaques: a model of simian

immunodeficiency virus-*Mycobacterium* coinfection. Infect. Immun. 2002; 70:869–877. [PubMed: 11796622]

8. Orme I. Adaptive immunity to mycobacteria. Curr. Opin. Microbiol. 2004; 7:58–61. [PubMed: 15036141]

9. Cooper AM, Khader SA. The role of cytokines in the initiation, expansion, and control of cellular immunity to tuberculosis. Immunol. Rev. 2008; 226:191–204. [PubMed: 19161425]

10. Flynn JL, Chan J, Triebold KJ, Dalton DK, Stewart TA, Bloom BR. An essential role for interferon γ in resistance to *Mycobacterium tuberculosis* infection. J. Exp. Med. 1993; 178:2249–2254. [PubMed: 7504064]

11. Yao S, Huang D, Chen CY, Halliday L, Zeng G, Wang RC, Chen ZW. Differentiation, distribution and γδ T cell-driven regulation of IL-22-producing T cells in tuberculosis. PLoS Pathog. 2010; 6:e1000789. [PubMed: 20195465]

12. Gambón-Deza F, Pacheco Carracedo M, Cerdá Mota T, Montes Santiago J. Lymphocyte populations during tuberculosis infection: Vβ repertoires. Infect. Immun. 1995; 63:1235–1240. [PubMed: 7890378]

13. Jacobsen M, Detjen AK, Mueller H, Gutschmidt A, Leitner S, Wahn U, Magdorf K, Kaufmann SH. Clonal expansion of CD8^{+} effector T cells in childhood tuberculosis. J. Immunol. 2007; 179:1331–1339. [PubMed: 17617626]

14. Tully G, Kortsik C, Höhn H, Zehbe I, Hitzler WE, Neukirch C, Freitag K, Kayser K, Maeurer MJ. Highly focused T cell responses in latent human pulmonary *Mycobacterium tuberculosis* infection. J. Immunol. 2005; 174:2174–2184. [PubMed: 15699149]

15. Du G, Qiu L, Shen L, Sehgal P, Shen Y, Huang D, Letvin NL, Chen ZW. Combined megaplex TCR isolation and SMART-based real-time quantitation methods for quantitating antigen-specific T cell clones in mycobacterial infection. J. Immunol. Methods. 2006; 308:19–35. [PubMed: 16403511]

16. Shen Y, Zhou D, Qiu L, Lai X, Simon M, Shen L, Kou Z, Wang Q, Jiang L, Estep J, et al. Adaptive immune response of Vγ2Vδ2^{+} T cells during mycobacterial infections. Science. 2002; 295:2255–2258. [PubMed: 11910108]

17. Shen Y, Shen L, Sehgal P, Zhou D, Simon M, Miller M, Enimi EA, Henckler B, Chalifoux L, Sehgal N, et al. Antiretroviral agents restore *Mycobacterium*-specific T cell immune responses and facilitate controlling a fatal tuberculosis-like disease in macaques coinfected with simian immunodeficiency virus and *Mycobacterium* bovis BCG. J. Virol. 2001; 75:8690–8696. [PubMed: 11507214]

18. Chen CY, Huang D, Wang RC, Shen L, Zeng G, Yao S, Shen Y, Halliday L, Fortman J, McAllister M, et al. A critical role for CD8 T cells in a nonhuman primate model of tuberculosis. PLoS Pathog. 2009; 5:e1000392. [PubMed: 19381260]

19. Ali Z, Shao L, Halliday L, Reichenberg A, Hintz M, Jomaa H, Chen ZW. Prolonged (*E*)-4-hydroxy-3-methyl-but-2-enyl pyrophosphate-driven antimicrobial and cytotoxic responses of pulmonary and systemic Vγ2Vδ2 T cells in macaques. J. Immunol. 2007; 179:8287–8296. [PubMed: 18056373]

20. Huang D, Shen Y, Qiu L, Chen CY, Shen L, Estep J, Hunt R, Vasconcelos D, Du G, Aye P, et al. Immune distribution and localization of phosphoantigen-specific Vγ2Vδ2 T cells in lymphoid and nonlymphoid tissues in *Mycobacterium tuberculosis* infection. Infect. Immun. 2008; 76:426–436. [PubMed: 17923514]

21. Lai X, Shen Y, Zhou D, Sehgal P, Shen L, Simon M, Qiu L, Letvin NL, Chen ZW. Immune biology of macaque lymphocyte populations during mycobacterial infection. Clin. Exp. Immunol. 2003; 133:182–192. [PubMed: 12869023]

22. Wei H, Wang R, Yuan Z, Chen CY, Huang D, Halliday L, Zhong W, Zeng G, Shen Y, Shen L, et al. DR*W201/P65 tetramer visualization of epitope-specific CD4 T cell during *M. tuberculosis* infection and its resting memory pool after BCG vaccination. PLoS ONE. 2009; 4:e6905. [PubMed: 19730727]

23. Chen ZW, Li Y, Zeng X, Kuroda MJ, Schmitz JE, Shen Y, Lai X, Shen L, Letvin NL. The TCR repertoire of an immunodominant CD8^{+} T lymphocyte population. J. Immunol. 2001; 166:4525–4533. [PubMed: 11254709]

24. Gallagher RE, Yeap BY, Bi W, Livak KJ, Beaubier N, Rao S, Bloomfield CD, Appelbaum FR, Tallman MS, Slack JL, Willman CL. Quantitative real-time RT-PCR analysis of PML-RARα mRNA in acute promyelocytic leukemia: assessment of prognostic significance in adult patients from intergroup protocol 0129. Blood. 2003; 101:2521–2528. [PubMed: 12468436]

25. Livak KJ, Schmittgen TD. Analysis of relative gene expression data using real-time quantitative PCR and the $2^{-\Delta\Delta C(T)}$ method. Methods. 2001; 25:402–408. [PubMed: 11846609]

26. Semighini CP, Marins M, Goldman MH, Goldman GH. Quantitative analysis of the relative transcript levels of ABC transporter Atr genes in *Aspergillus nidulans* by real-time reverse transcription-PCR assay. Appl. Environ. Microbiol. 2002; 68:1351–1357. [PubMed: 11872487]

27. Zhou D, Shen Y, Chalifoux L, Lee-Parritz D, Simon M, Sehgal PK, Zheng L, Halloran M, Chen ZW. *Mycobacterium* bovis bacille Calmette-Guérin enhances pathogenicity of simian immunodeficiency virus infection and accelerates progression to AIDS in macaques: a role of persistent T cell activation in AIDS pathogenesis. J. Immunol. 1999; 162:2204–2216. [PubMed: 9973496]

28. Chen ZW, Shen L, Regan JD, Kou Z, Ghim SH, Letvin NL. The T cell receptor gene usage by simian immunodeficiency virus gag-specific cytotoxic T lymphocytes in rhesus monkeys. J. Immunol. 1996; 156:1469–1475. [PubMed: 8568249]

29. Chen ZW, Kou ZC, Lekutis C, Shen L, Zhou D, Halloran M, Li J, Sodroski J, Lee-Parritz D, Letvin NL. T cell receptor Vβ repertoire in an acute infection of rhesus monkeys with simian immunodeficiency viruses and a chimeric simian-human immunodeficiency virus. J. Exp. Med. 1995; 182:21–31. [PubMed: 7540651]

30. Shen Y, Shen L, Sehgal P, Huang D, Qiu L, Du G, Letvin NL, Chen ZW. Clinical latency and reactivation of AIDS-related mycobacterial infections. J. Virol. 2004; 78:14023–14032. [PubMed: 15564509]
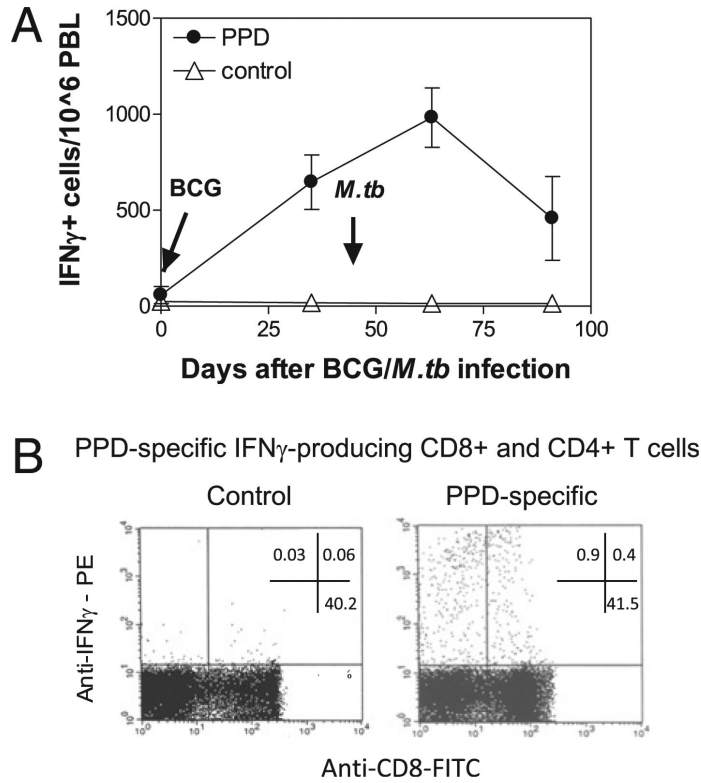
FIGURE 1.
PPD-specific T effector cells producing IFN-**γ** upon stimulation were detectable after BCG vaccination and *M. tuberculosis* infection. Shown are ELISPOT data (*A*) indicating IFN-γ[+] cellular responses in PBMCs after BCG vaccination and *M. tuberculosis* infection of juvenile Indian rhesus macaques (*A*) and representative flow histogram data (*B*) displaying PPD-specific IFN-γ^{+} CD8^{+} and CD8^{−} (CD4^{+}) T cells measured by intracellular cytokine staining after stimulation with PPD or medium control. Data were gated on CD3, with percentages indicated in quadruples. Both IFN-γ^{+} CD8^{+} and CD4^{+} T cell populations were purified by flow cytometry sorting (15). ELSPOT data are mean values with SEM from four macaques.

Mm3055; CD4+ T-cell clones

#	Vβ-Jβ clone	Vβ	D+N	Jβ	CDR3
55-1	Vβ3Jβ2.7	CASS	LLGVSD	EQYFG	10
55-2	Vβ3Jβ1.2	CASS	TLEGE	NYDYTFG	11
55-3	Vβ3Jβ1.3	CASS	LS	GNTVYFG	8
55-4	Vβ3Jβ1.6	CASS	LLGGD	NSPLHFG	11
55-5	Vβ3Jβ2.2	CASS	SHH	NTAQLFF	9
55-6	Vβ3Jβ2.3	CASS	FNRQDC	TDPQYFG	12
55-7	Vβ3Jβ2.4	CASR	GRGTD	TQYFG	9
55-8	Vβ4Jβ1.3	CSV	DTGTPHS	GNTVYFG	13
55-9	Vβ4Jβ1.4	CSV	RDREA	EKLFFG	9
55-10	Vβ4Jβ1.5	CSV	GGT	NQPQYFG	8
55-11	Vβ4Jβ2.3	CSV	EAG	DPQYFG	7
55-12	Vβ4Jβ2.5	CSV	XKTRDIQ	ETQYFG	11
55-13	Vβ4Jβ2.7	CG	XQAPQN	YEQYFG	10
55-14	Vβ6Jβ1.1	CASS	LAGLG	TEAFFG	10
55-15	Vβ6Jβ1.3	CASS	QTEMR	NTVYFG	10
55-16	Vβ6Jβ1.5	CASS	LEGD	QPQYFG	9
55-17	Vβ6Jβ2.4	CASS	LGGRDSWR	NTQYFG	13
55-18	Vβ6Jβ2.6	CASS	LGATWGFNGS	GASVLTFG	17
55-19	Vβ8Jβ1.6	CASS	LPL	YNSPLYFG	10
55-20	Vβ8Jβ2.2	CASS	LGSGTH	AQLFFG	11
55-21	Vβ8Jβ2.3	CASS	YGRR	TDPQYFG	10
55-22	Vβ10Jβ1.2	CASS	TYWTGN	DYTFG	10
55-23	Vβ10Jβ1.4	CASS	TR	EKLFFG	7
55-24	Vβ12Jβ1.3	CASR	AT	GNTVYFG	8
55-25	Vβ13Jβ2.6	CASS	ESGS	GASVLTFG	11
55-26	Vβ14Jβ2.3	CASS	FNRQDC	TDPQYFG	12
55-27	Vβ14Jβ2.7	CASS	LLGVSD	EQYFG	9
55-28	Vβ16Jβ1.4	CASS	PGYEGF	EKLFFG	11
55-29	Vβ16Jβ2.4	CASS	QEEGV	QNTQYFG	11
55-30	Vβ17Jβ1.2	CAS	XHRTGD	DYTFG	9

Mm3050; CD4+ T-cell clones

#	Vβ-Jβ clone	Vβ	D+N	Jβ	CDR3
50-1	Vβ13.2Jβ2.7	CASS	ESMRG	YEQYFG	10
50-2	Vβ18Jβ2.7	CAW	SEEGDNS	YEQYFG	11
50-3	Vβ21Jβ2.2	CASS	LGGGD	TAQLFFG	12
50-4	Vβ5Jβ2.7	CASS	SGLGVT	SYEQYFG	12
50-5	Vβ6Jβ1.3	CASS	LHKRGS	GNTVYFG	12
50-6	Vβ6Jβ1.4	CASS	LDAGGG	EKLFFG	11
50-7	Vβ6Jβ2.4	CAS	RKRDS	QNTQYFG	10
50-8	Vβ7Jβ2.7	CASS	QEGTGF	SYEQYFG	12
50-9	Vβ8Jβ1.2	CASS	FPTGC	YDYTFG	10
50-10	Vβ8Jβ1.5	CASR	QGY	QPQYFG	8
50-11	Vβ8Jβ2.4	CASR	KRDS	QNTQYFG	10
50-12	Vβ8Jβ1.1	CASS	LAGP	EAFFG	8
50-13	Vβ20Jβ1.3	CASS	LHKRGS	GNTVYFG	12
50-14	Vβ20Jβ2.2	CASS	RGRDRGIV	AQLFFG	13
50-15	Vβ23Jβ1.2	CAS	TKKGQGN	DYTFG	10
50-16	Vβ5Jβ1.3	CASS	LSEAGQGGS	GNTVYFG	15
50-17	Vβ6Jβ2.7	CASS	KGRK	SYEQYFG	9
50-18	Vβ6Jβ2.3	CASR	LGGL	DPQYFG	9
50-19	Vβ6Jβ2.5	CASS	RGLDQ	ETQYFG	10
50-20	Vβ8Jβ1.3	CASS	LSEAGQGGS	GNTVYFG	15
50-21	Vβ10Jβ2.3	CASS	SEGQP	TDPQYFG	11
50-22	Vβ13.2Jβ2.3	CAS	KVRG	TDPQYFG	9
50-23	Vβ16Jβ2.7	CASS	SAGQA	EQYFG	9
50-24	Vβ20Jβ2.7	CASS	RLGTGW	EQYFG	10
50-25	Vβ23Jβ1.2	CASS	GTA	NYDYTFG	9

Mm2995; CD4+ T-cell clones

#	Vβ-Jβ clone	Vβ	D+N	Jβ	CDR3
95-1	Vβ3.5Jβ2.7	CASS	LTGGL	SYEQYFG	11
95-2	Vβ4Jβ1.2	CSV	LRGFDT	YDYTFG	11
95-3	Vβ4Jβ2.5	CSV	DTRDWGELVG	TQYFG	14
95-4	Vβ4Jβ2.6	CSV	DTGTGGSS	GASVLTFG	14
95-5	Vβ6Jβ1.1	CASS	LLVR	NTEAFFG	10
95-6	Vβ7Jβ1.3	CAS	PKTGTPHS	GNTVYFG	13
95-7	Vβ7Jβ1.4	CAS	QGQV	TNEKLFFG	10
95-8	Vβ7Jβ2.1	CAS	THTGLGDHG	EQFFG	12
95-9	Vβ8Jβ1.2	CASS	PGGSD	YDYTFG	10
95-10	Vβ8Jβ1.4	CAS	RPGQG	EKLFFG	9
95-11	Vβ8Jβ2.3	CASN	LISGFL	TDPQYFG	12
95-12	Vβ8Jβ2.5	CASS	LGQG	ETQYFG	9
95-13	Vβ14Jβ2.5	CASS	PRGR	ETQYFG	9
95-14	Vβ16Jβ1.2	CASS	QREGV	NYDYTFG	11
95-15	Vβ18Jβ1.5	CA	WGGGRR	NQPQYFG	11
	CD8+ T-cell clones				
95-16	Vβ19Jβ1.5	CASS	IYG	QPQYFG	8
95-17	Vβ20Jβ2.4	CASS	QGIS	QNTQYFG	9
95-18	Vβ23Jβ2.5	CASS	EATLWGELVG	TQYFG	14
95-19	Vβ8.Jβ2.3	CASS	NLISGFL	TDPQYFG	12
95-20	Vβ11Jβ2.3	CASS	XDRTGV	DPQYFG	11
95-21	Vβ19Jβ1.5	CASS	ITGGS	NQPQYFG	11
95-22	Vβ20Jβ2.7	CASS	LGAG	SYEQYFG	10

Mm2823; CD4+ T-cell clones

#	Vβ-Jβ clone	Vβ	D+N	Jβ	CDR3
23-1	Vβ1Jβ2.7	CASS	PGLGTT	YEQYFG	11
23-2	Vβ15Jβ1.6	CAS	NSAGRE	NSPLHFG	11
23-3	Vβ7Jβ2.3	CAS	QSAGAG	DPQYFG	10
23-4	Vβ8Jβ2.2	CAS	KPSRGAR	TAQLFFG	12
23-5	Vβ13.2Jβ2.1	CASS	DQDYG	EQFFG	9
23-6	Vβ13.2Jβ2.6	CASS	ESGS	GASVLTFG	11
23-7	Vβ19Jβ1.5	CASS	IYG	QPQYFG	8
23-8	Vβ20Jβ2.4	CASS	QGIS	QNTQYFG	10
23-9	Vβ20Jβ2.3	CASS	QRN	PQYFG	7
23-10	Vβ24Jβ2.2	CASS	ARDRD	TAQLFFG	11
	CD8+ T-cell clones				
23-11	Vβ1Jβ1.4	CASS	LAKGGYY	EKLFFG	12
23-12	Vβ1Jβ2.7	CASS	PRGG	YEQYFG	10
23-13	Vβ8Jβ1.4	CASR	PGPGVY	EKLFFG	11
23-14	Vβ9Jβ1.4	CASS	QGQVTN	EKLFFG	11
23-15	Vβ11Jβ2.3	CASS	CIGTGV	DPQYFG	11
23-16	Vβ12Jβ2.6	CASS	ESGDRGLS	GASVLTFG	15
23-17	Vβ13Jβ1.3	CASS	EGLR	NTVYFG	9

Mm2762; CD4+ T-cell clones

#	Vβ-Jβ clone	Vβ	D+N	Jβ	CDR3
62-1	Vβ1Jβ1.3	CASS	QGRIA	GNTVYFG	11
62-2	Vβ7Jβ1.6	CASS	HNSRWA	NSPLYFG	12
62-3	Vβ24Jβ1.4	CASS	KLKAG	NEKLFFG	11
62-4	Vβ8Jβ1.2	CASS	NNRDD	DYTFG	9
	CD8+ T-cell clones				
62-5	Vβ7Jβ2.4	CASS	QGIS	QNTQYFG	10
62-6	Vβ8Jβ1.2	CASS	LNRDD	DYTFG	9
62-7	Vβ8Jβ2.3	CAS	NLISGFL	TDPQYFG	12
62-8	Vβ8Jβ2.1	CASS	GEG	NEQFFG	8
62-9	Vβ12Jβ2.1	CAS	IEGLGGY	NEQFFG	11

FIGURE 2.
PPD-specific CD4^{+} and CD8^{+} T effector clones employed diverse TCR Vβ repertoires; 30–33% of IFN-γ^{+}CD4^{+} T cell clones from three *M. tuberculosis*-infected macaques expressed TCR bearing a conserved residue leucine in CDR3. Shown are TCR sequences in V-D-J junctional regions for CD4^{+} and CD8^{+} T cell clones. Clone numbers (#) from TCR isolation, clone ID (Vβ-Jβ usage), amino acid sequences of Vβ (3′ end), D+N and Jβ, and CDR3 lengths are indicated. CDR3 lengths were defined as previously described (23, 27, 29). Note a conserved residue leucine that is bold and underlined in the TCR N+D region of the clones isolated from macaques 3055, 2995, and 3050. To maximize the detection of *M. tuberculosis*-specific IFN-γ[+] T effector cells using the ICS method, PBLs collected at weeks 5 or 7 after *M. tuberculosis* infection were stimulated with PPD, stained for IFN-γ and surface CD3, CD4, and CD8, and subjected to isolation of IFN-γ^{+} CD4^{+} or CD8^{+} T effector cells by flow cytometry sorting as we previously described (15, 23). Thirty to 55% of the

clones were isolated from PBLs obtained at both weeks 5 and 7 after *M. tuberculosis* infection.
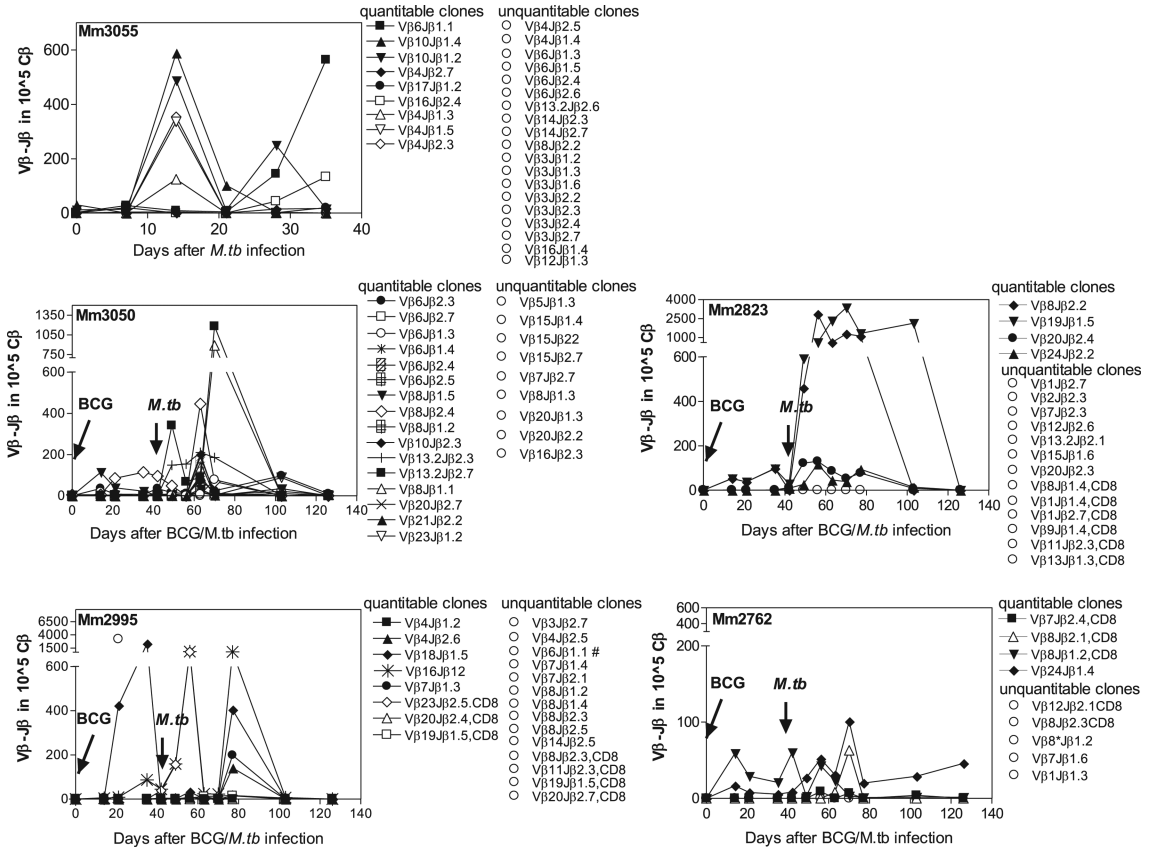
FIGURE 3.
Many Ag-specific IFN-γ⁺ CD4⁺ and few CD8⁺ T effector cells emerged as dominant clones during mycobacterial infections and underwent major recall expansion after pulmonary *M. tuberculosis* infection of BCG-vaccinated macaques. Shown are the frequencies for individual clonotypic TCR clones in the blood T cell pool after i.v. BCG vaccination (four macaques) and pulmonary *M. tuberculosis* infection (five macaques). Data are expressed as clonotypic TCR copy numbers in 10^5 total TCR β (Cβ) transcripts. The time for BCG vaccination or *M. tuberculosis* infection is pointed to by an arrow in each panel. CD8⁺ T effector clones were indicated; otherwise, they were CD4⁺ T effector clones. Note that the quantitatable and unquantitatable TCR clones are grouped, respectively, for each macaque. The real-time quantitation method confers a detection limit for TCR transcripts corresponding to 10^{-5} Ag-specific T cells (15). Most clones became unquantitatable around the time point of anti-TB chemotherapy (denoted by drug), which might be attributed to the vaccine-induced immune control of acute *M. tuberculosis* infection. Note that Vβ23Jβ2.5 (◇) and Vβ16Jβ1.2 (*) clones from macaque 2995 exhibited similar frequencies early after *M. tuberculosis* infection, whereas Vβ16Jβ1.1 clone (marked by #) became unquantitatable after *M. tuberculosis* infection. The low-level recall clonal expansion for macaque 2762 appeared to correlate with extremely low bacterial burden after *M. tuberculosis* infection (16).
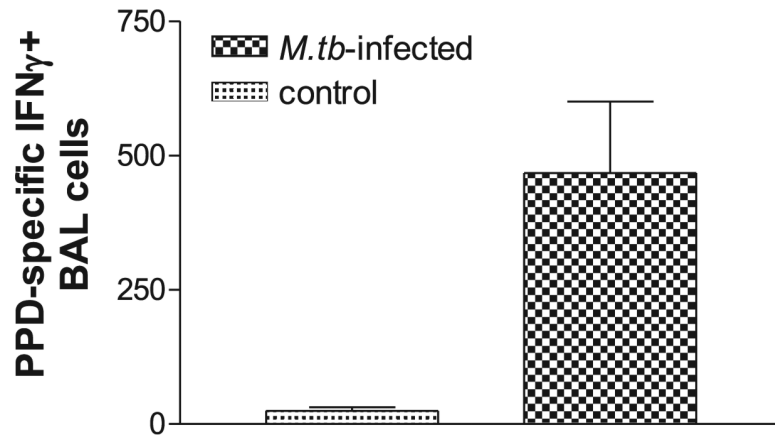
FIGURE 4.
PPD-specific IFN-γ–producing cells were detectable in the airway in *M. tuberculosis*-infected macaques. Shown are ELSPOT data for PPD-specific IFN-γ^+ cell responses in BAL fluid collected from three *M. tuberculosis*-infected macaques at day 41 after the infection, as well as from three uninfected healthy macaques (control). Data were subtracted from values of medium alone and expressed as IFN-γ^+ cells in 10^6 BAL cells. From Student *t* test analysis, $p < 0.05$ between the groups.

Mm3055; Clones detected both in blood (PBL) and airway (BAL)

Clones	PBL D0	PBL D7	BAL D8	PBL D14	BAL D14	PBL D21	BAL D25	PBL D28	BAL D41
Vβ10Jβ1.4	3	0	7	588	354	102	46	3.5	6
Vβ10Jβ1.2	1	0	8	487	3	11	228	250	0
Vβ6Jβ1.1	3	0	2	9	4	4	6	144	136
Vβ4Jβ1.5	0	0	0	335	0	0	0	0	337
Vβ4Jβ2.3	0	0	0	354	0	0	0	0	55
Other clones			0		0		0		0

Mm3050; Clones detected both in blood (PBL) and airway (BAL)

Clones	PBL D0	PBL D7	BAL D8	PBL D21	BAL D25	PBL D28	PBL D61	BAL D61
Vβ13.2Jβ2.3	1	149	29	210	103	186	0	0
Vβ13.2Jβ2.7	1	341	41	90	184	1181	0	103
Vβ15Jβ2.2	0	0	1	0	6	0	0	0
Vβ20Jβ2.2	2	1	3	0	0	1	0	12
Vβ20Jβ2.7	5	7	38	90	11	12	0	0
Vβ21Jβ2.2	1	2	1	97	468	4	0	31
Vβ23Jβ1.2	5	2	2	18	7	3	88	0
Vβ6Jβ2.3	35	16	151	72	6	25	97	0
Vβ6Jβ2.4	5	10	2	189	9	13	0	4
Vβ8Jβ2.4	96	49	108	446	1031	69	0	284
Vβ8Jβ1.2	2	2	6	163	2	1	0	288
other clones			0		0			0

Mm2995; Clones detected both in blood (PBL) and airway (BAL)

Clones	PBL D0	PBL D7	BAL D8	PBL D14	BAL D14	PBL D21	BAL D25	PBL D35	BAL D41	BAL D61
Vβ18Jβ1.5	0	0	2.2	34	27	0	5	404	2047	0
Vβ16Jβ1.2	0	0	5.9	33	40	0	18	775	5384	9
Vβ23Jβ2.5	38	156	0	787	0	12	0	16	0	0
Vβ4Jβ1.2	0	0	1	0	18	0	1	0	0	0
Vβ4Jβ2.6	0	0	3.9	9	81	0	11	141	3716	1.0
Vβ7Jβ1.3	0	0	5.5	0	41	0	9	198	2600	1.7
Others			0		0		0		0	0

Mm2823; Clones detected both in blood (PBL) and airway (BAL)

Clones	PBL D0	PBL D7	BAL D8	PBL D14	BAL D14	PBL D21	BAL D25	PBL D35	BAL D41	BAL D61
Vβ20Jβ2.4	12	121	147	130	65	87	108	77	147	466
Vβ24Jβ2.2	9	27	204	118	219	46	103	95	83	396
Vβ8Jβ2.2	0	459	378	2855	1286	613	369	1120	410	860
Vβ19Jβ1.5	28	592	40	606	24	2327	57	1332	27	127
Other clones			0		0		0		0	0

Mm2762; Clones detected both in blood (PBL) and airway (BAL)

Clones	PBL D0	PBL D7	BAL D8	PBL D14	BAL D14	PBL D21	BAL D25	PBL D35	BAL D41	BAL D61
Vβ8Jβ1.2	60	3	20	43	190	23	20	10	10	2
Vβ7Jβ2.4	0	0	0	10	9	0	0	0	0	0
other clones			0		0		0		0	0

FIGURE 5.

PPD-specific CD4^{+} and CD8^{+} T cell clones readily trafficked to the airway after *M. tuberculosis* infection, and some of them continuously accumulated in lungs even after they became undetectable in the circulation. Shown are the frequencies (clonotypic TCR copy numbers in 10^5 total TCR β (Cβ) transcripts) of clonotypic TCR clones detected both in blood (PBLs) and airway (BAL) at different days (D) after *M. tuberculosis* infection of macaques. Data for BAL are highlighted in light black. Only those dominant clones quantitatable in PBLs were subjected to real-time quantitation in BAL samples due to the limited numbers of BAL cells.

Mm22794; Clones detected both in blood (PBL) and airway (BAL) after 2nd BCG

Clones	PBL # D-21	BAL # D-21	PBL # D14	BAL # D14	PBL # D34	BAL # D34	PBL D61	BAL D61	PBL D129	BAL D129	PBL D165	BAL D165
Vβ9Jβ2.2	0	0	547	384	0	2	344	1	4	1	18	0
Vβ9Jβ1.1	0	0	0	0	4334	44	1329	567	2	1648	0	0
Vβ20Jβ1.3	3	0	48	0	8229	1160	81	269	1	0	21	38
Vβ20Jβ2.7	2	0	485	9	2	47	3460	0	27	0	594	0

Mm12485; Clones detected both in blood (PBL) and airway (BAL) after 2nd BCG

Clones	PBL # D-21	BAL # D-21	PBL # D14	BAL # D14	PBL # D34	BAL # D34	PBL D61	BAL D61	PBL D129	BAL D129	PBL D165	BAL D165
Vβ6Jβ2.4	289	39	243	344	325	278	223	594	560	178	368	862
Vβ9Jβ2.4	132	159	2609	1171	4677	71	720	318	1011	509	1046	400
Vβ21Jβ2.4	81	0	172	21	221	54	121	241	10	27	30	32

FIGURE 6.
PPD-specific IFN-γ–producing CD4^{+} T cell clones readily trafficked to the airway as well after the second i.v. BCG vaccination. Shown are the frequencies of clonotypic TCR clones detected both in PBLs and BAL fluid after the second BCG vaccination of macaques. The first BCG vaccination was done 4 mo earlier. The primary BCG infection is usually resolved within 2 mo after the first i.v. BCG inoculation. No BCG mycobacteria were detected in BAL samples after the second BCG vaccination. # indicates that no BCG bacteria were isolated from the blood and BAL fluid collected from denoted times (#) after the second BCG vaccination. BCG CFUs were measured using 7H10 agar plates (16). There were no or few neutrophils seen over time in BAL fluid.
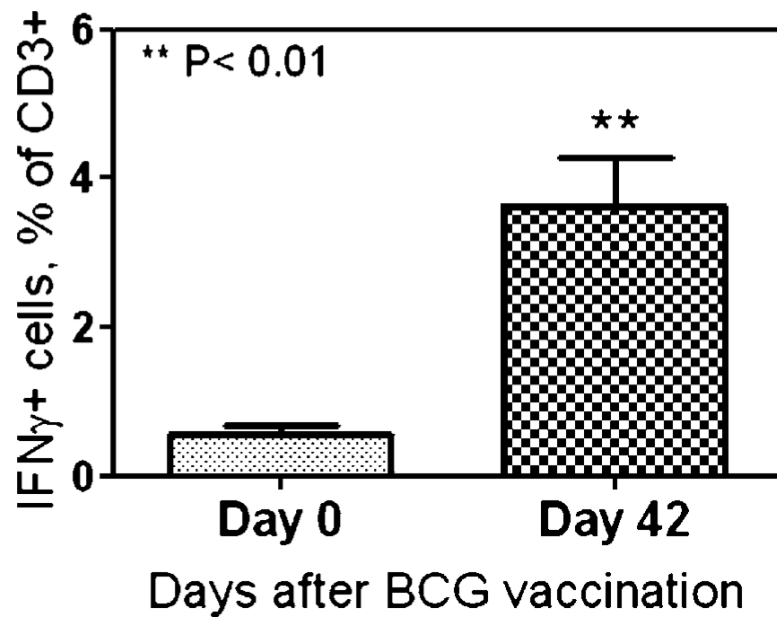
FIGURE 7.
Accumulation of T effector cells in the airway was also induced by intradermal BCG vaccination. Shown are ICS data indicating mean frequencies of PPD-specific IFN-γ^+ T cells in BAL cells from four rhesus macaques vaccinated intradermally with BCG (18).
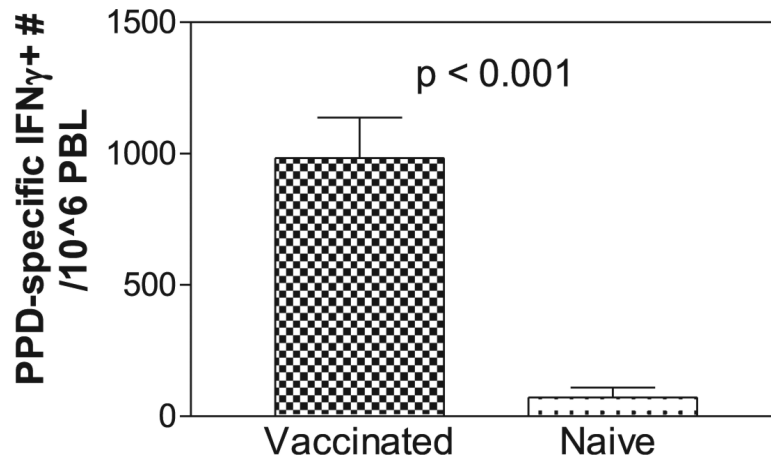
FIGURE 8.
Rapid major expansion of BCG-primed T effector cells after *M. tuberculosis* infection was associated with protection against fatal TB in juvenile Indian rhesus macaques. Shown are mean comparative ELI-SPOT data from BCG-vaccinated and naive control groups at 3 wk after *M. tuberculosis* infection. All vaccinated macaques survived with very low-level *M. tuberculosis* burden, whereas all naive controls died (16).